Available online at www.sciencedirect.com
SCIENCE DIRECT®
Tectonophysics 407 (2005) 257–268
TECTONOPHYSICS
www.elsevier.com/locate/tecto

Late Quaternary faulting along the western margin of the Poronaysk Lowland in central Sakhalin, Russia

Hiroyuki Tsutsumi [a,*], Yasuhiro Suzuki [b], Andrei I. Kozhurin [c], Mihail I. Strel'tsov [d], Takeyuki Ueki [e], Hideaki Goto [f], Koji Okumura [g], Rustam F. Bulgakov [d], Hiroyuki Kitagawa [h]

[a] *Department of Geophysics, Graduate School of Science, Kyoto University, Kyoto 606-8502, Japan*
[b] *Research Center for Seismology, Volcanology and Disaster Mitigation, Graduate School of Environmental Studies, Nagoya University, Nagoya 464-8602, Japan*
[c] *Geological Institute, Russian Academy of Sciences, Moscow 109017, Russia*
[d] *Institute of Marine Geology and Geophysics, Russian Academy of Sciences, Yuzhno-Sakhalinsk 693002, Russia*
[e] *Institute of Geology and Geoinformation, Geological Survey of Japan, Tsukuba 305-8567, Japan*
[f] *Department of Geography, College of Human Development and Culture, Fukushima University, Fukushima 960-1296, Japan*
[g] *Department of Geography, Graduate School of Letters, Hiroshima University, Higashi-Hiroshima 739-8522, Japan*
[h] *Department of Earth and Environmental Sciences, Graduate School of Environmental Studies, Nagoya University, Nagoya 464-8601, Japan*

Received 11 February 2005; received in revised form 9 August 2005; accepted 15 August 2005
Available online 19 September 2005

Abstract

Sakhalin Island straddles an active plate boundary between the Okhotsk and Eurasian plates. South of Sakhalin, this plate boundary is illuminated by a series of M_w 7–8 earthquakes along the eastern margin of the Sea of Japan. Although this plate boundary is considered to extend onshore along the length of Sakhalin, the location and convergence rate of the plate boundary had been poorly constrained. We mapped north-trending active faults along the western margin of the Poronaysk Lowland in central Sakhalin based on aerial photograph interpretation and field observations. The active faults are located east of and parallel to the Tym–Poronaysk fault, a terrane boundary between Upper Cretaceous and Neogene strata; the active faults appear to have reactivated the terrane boundary at depth in Quaternary time. The total length of the active fault zone on land is about 140 km. Tectonic geomorphic features such as east-facing monoclinal and fault scarps, back-tilted fluvial terraces, and numerous secondary faults suggest that the faults are west-dipping reverse faults. Assuming the most widely developed geomorphic surface in the study area formed during the last glacial maximum at about 20 ka based on similarities of geomorphic features with those in Hokkaido Island, we obtain a vertical component of slip rate of 0.9–1.4 mm/year. Using the fault dip of 30–60°W observed at an outcrop and trench walls, a net slip rate of 1.0–2.8 mm/year is obtained. The upper bound of the estimate is close to a convergence rate across the Tym–Poronaysk fault based on GPS measurements. A trenching study across the fault zone dated the most recent faulting event at 3500–4000 years ago. The net slip associated with this event is estimated at about 4.5 m. Since the last faulting event, a minimum of 3.5 m of strain, close to the strain released during the last event, has accumulated along the central portion of the active strand of the Tym–Poronaysk fault.

Keywords: Sakhalin; Tym–Poronaysk fault; Active faulting; Paleoseismology; Slip rate; Plate boundary

* Corresponding author. Tel.: +81 75 753 3942; fax: +81 75 753 4291.
E-mail address: tsutsumh@kugi.kyoto-u.ac.jp (H. Tsutsumi).

0040-1951/$ - see front matter © 2005 Elsevier B.V. All rights reserved.
doi:10.1016/j.tecto.2005.08.007

1. Introduction

Sakhalin Island lies on an active plate boundary between the Okhotsk and Eurasian plates (Fig. 1). South of Sakhalin, this plate boundary is located offshore along the eastern side of the Sea of Japan where a series of M_w 7–8 earthquakes occurred in the last century, including the devastating 1983 M_w 7.7 Sea of Japan and 1993 M_w 7.7 Hokkaido Nansei-oki earthquakes. Farther north, this plate boundary is considered to extend onshore along the length of Sakhalin (Seno et al., 1996). However, the location and convergence rate of the plate boundary in Sakhalin has been poorly constrained by geologic data.

A study by a French–Russian group (Fournier et al., 1994) described the major faults of this plate boundary in Sakhalin based on interpretation of satellite images, structural analysis of the faults, and studies of instrumental seismicity. The major faults identified were the Tym–Poronaysk fault that extends northward from the southwest peninsula west of Aniva Bay to the west-central part of the island and the Ekhabi–Pil'tun fault in northeast Sakhalin (Fig. 2). Although these faults were

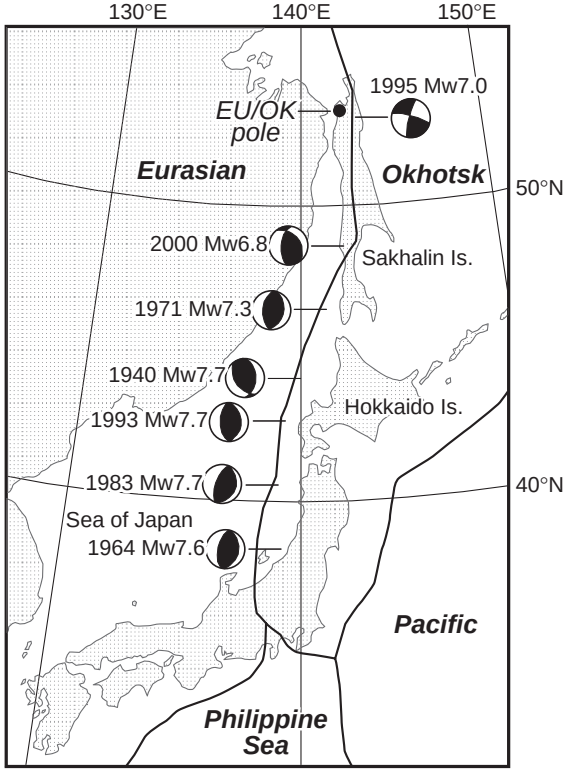

Fig. 1. Plate tectonic framework of the Japanese and Sakhalin Islands showing plate geometry after Seno et al. (1996) and focal mechanism solutions of large earthquakes along the Okhotsk and Eurasian plate boundary since 1940 after Katsumata et al. (2004). The Eurasian/Okhotsk Euler pole is from Seno et al. (1996).

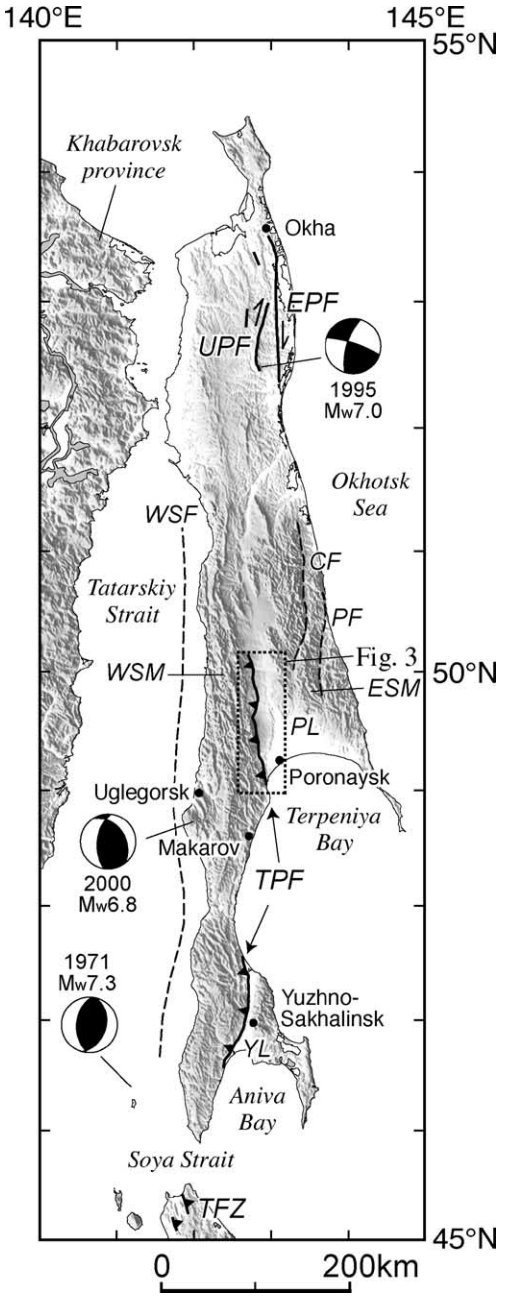

Fig. 2. Distribution of active faults (solid lines) and historical large earthquakes in and around Sakhalin. Active faults in Sakhalin are from Suzuki et al. (2000) and Tsutsumi et al. (2000), and those in Hokkaido south of the Soya Strait are from Ikeda et al. (2002). Focal mechanism solutions for historical earthquakes are from Katsumata et al. (2004). Abbreviations for active faults are EPF, Ekhabi–Pil'tun fault; TFZ, Teshio fault zone; TPF, Tym–Poronaysk fault; UPF, Upper Pil'tun fault. Abbreviations for physiographic features are ESM, East Sakhalin Mountains; PL, Poronaysk Lowland; WSM, West Sakhalin Mountains; YL, Yuzhno–Sakhalinsk Lowland. Dashed lines denote inactive or uncertain faults from Fournier et al. (1994). CF, Central fault; PF, Pribrezhnaya fault; WSF, West Sakhalin fault. Shaded relief map was drawn with the GMT software (Wessel and Smith, 1998).

assumed to be active, no geologic or geomorphic evidence for recent activity was presented.

Seismic hazards in Sakhalin had not been seriously considered until the 1995 M_w 7.0 Neftegorsk earthquake in northern Sakhalin that claimed about 2000 casualties (Ivashchenko et al., 1997). Since then, Russian and Japanese scientists have made extensive efforts to identify potential seismic sources and characterize their seismic risk. Suzuki et al. (2000) presented a preliminary active fault map of Sakhalin and described the distribution and sense of movement of the active faults. Tsutsumi et al. (2000) conducted geomorphic mapping and paleoseismic trenching in northeastern Sakhalin including the fault that ruptured during the 1995 Neftegorsk earthquake. Bulgakov et al. (2002) compiled geologic data for active faults in northeastern Sakhalin and presented geomorphic and paleoseismic data in central and southern Sakhalin. In this paper, we describe active faulting along the western margin of the Poronaysk Lowland in central Sakhalin, which had not been discussed in detail in previous papers. We discuss distribution, sense of movement, slip rate, and paleoseismology of the fault zone based on aerial photograph interpretation conducted during 1997 and 2000 and field observation in 1998. Our data have important implications not only for seismic hazard assessment in central Sakhalin but also for understating active tectonics along the Okhotsk and Eurasian plate boundary north of Hokkaido Island.

2. Regional setting

2.1. Geologic framework of Sakhalin

Sakhalin Island is located north of Hokkaido Island across the Soya Strait and east of the Khabarovsk province across the Tatarskiy Strait (Fig. 2). The island is about 1100 km long and as wide as 250 km near latitude 49°N, whereas it is only 30 km wide at latitude 48°N. Physiographically, the island can be divided into a south-central part characterized by mountain ranges and lowlands, and a northern part characterized by low-relief hills (Fig. 2). The southern and central portions of the island contain the East and West Sakhalin Mountains with the highest peak above 1600 m. These mountains consist of Mesozoic to Paleogene metamorphic and sedimentary rocks (Fournier et al., 1994). The lowlands between the mountains are called the Central Lowland filled with Quaternary deposits: the Yuzhno–Sakhalinsk Lowland north of Aniva Bay and Poronaysk Lowland north of Terpeniya Bay (Fig. 2). The northern part of the island is composed mainly of sedimentary rocks of Neogene age.

The geology and tectonics of Sakhalin are strongly controlled by north-trending faults (Rozhdestvenskiy, 1982; Fournier et al., 1994). The eastern margin of the West Sakhalin Mountains is bounded by the west-dipping Tym–Poronaysk fault for a distance of about 600 km. The eastern margin of the East Sakhalin Mountains is also bounded by several north-trending faults such as the Central and Pribrezhnaya faults. The northeastern part of the island is also cut by several north-trending faults, such as the Ekhabi–Pil'tun and Upper Pil'tun faults (Fig. 2). In addition to these onshore structures, the southwest coast of the island appears be bordered by the West Sakhalin fault parallel to the Tym–Poronaysk fault. Rozhdestvenskiy (1982) and Fournier et al. (1994) suggested that these north-trending faults were right-lateral strike-slip faults in Miocene time. Kimura et al. (1983) and Jolivet and Miyashita (1985) also documented transpressional deformation associated with right-lateral strike-slip motion along north-trending faults in Sakhalin and Hokkaido during the Oligocene and Miocene.

2.2. Distribution of active faults and historical seismicity in Sakhalin

Since 1997, we have interpreted aerial photographs at scales of 1:10,000 to 1:40,000 that cover about 50% of Sakhalin Island. For the rest of the island, we have interpreted satellite images. We have compiled a preliminary active fault map of Sakhalin at a scale of 1:500,000 (Fig. 2; Suzuki et al., 2000; Tsutsumi et al., 2000). This map shows two major zones of active deformation: a north-trending right-lateral strike-slip fault zone in northeastern Sakhalin and a north-trending reverse fault zone in central and southern Sakhalin. The faults at the eastern margin of the East Sakhalin Mountains show no evidence of late Quaternary movement.

The faults along the northeastern coast of Sakhalin include the Upper Pil'tun fault that ruptured during the 1995 Neftegorsk earthquake, and the Ekhabi–Pil'tun fault east of the surface rupture (Tsutsumi et al., 2000; Bulgakov et al., 2002). The 35-km-long, predominantly right-lateral strike-slip surface rupture appeared along the Upper Pil'tun fault during the 1995 earthquake (Shimamoto et al., 1996; Ivashchenko et al., 1997; Arefiev et al., 2000). The maximum displacement was about 8 m. Systematic right-lateral stream offsets as much as 80 m along the Upper Pil'tun fault

demonstrate that similar earthquakes have occurred repeatedly along the fault in the late Quaternary (Tsutsumi et al., 2000). Rogozhin (1996) identified stratigraphic evidence for prior earthquakes by trenching studies. The north-trending Ekhabi–Pil'tun fault extends for about 130 km. Right-lateral offsets of stream channels and lakeshores suggest that the Ekhabi–Pil'tun fault is also a right-lateral strike-slip fault. A 3-m-deep trench across the central portion of the fault exposed near vertical fault strands and contained geologic evidence for two episodes of prehistoric surface faulting. The most recent event occurred after 2950 B. C. and the penultimate earthquake occurred sometime between 5480 and 4780 B. C. (Tsutsumi et al., 2000).

The two active reverse fault zones in central and southern Sakhalin are each more than 100 km in length (Fig. 2). These active faults are located within 15 km east of and almost parallel to the Tym–Poronaysk fault, a west-dipping terrane boundary between Upper Cretaceous and Neogene strata that shows no evidence for late Quaternary movement (Fig. 3). A geologic cross-section by Rozhdestvenskiy (1982) suggested that the active faults appear to merge with and reactivate the terrane boundary fault. In the remainder of this paper, we call the active faults as the active strands of the Tym–Poronaysk fault and the terrane boundary fault as the Tym–Poronaysk terrane boundary fault. Although there is little geologic data in Terpeniya Bay, the reverse fault zones in central and southern Sakhalin may connect one another, as suggested by uplifted marine terraces and numerous flexural-slip faults, which are typically observed on the hanging wall side of active reverse faults (Yeats, 1986).

Sakhalin Island and the surrounding area have been seismically active in historic times, including the 1971 M_w 7.3 Moneron earthquake, 1995 Neftegorsk earthquake, and 2000 M_w 6.8 Uglegorsk earthquake (Fig. 2). The 1971 and 2000 earthquakes both show focal mechanism solutions of reverse faulting. Aftershocks and geodetic data suggest that a previously unidentified east-dipping fault ruptured during the 2000 Uglegorsk earthquake (Kogan et al., 2003). Instrumental seismicity suggests that the Tym–Poronaysk fault is active and has caused most of the inland earthquakes of Sakhalin. Focal mechanisms determined along the Tym–Poronaysk fault show reverse and right-lateral strike-slip motions (Fournier et al., 1994). GPS data indicate east–west shortening across the island and the convergence rate with right-lateral component of slip across the Tym–Poronaysk fault is estimated at about 3 mm/year (Kogan et al., 2003).

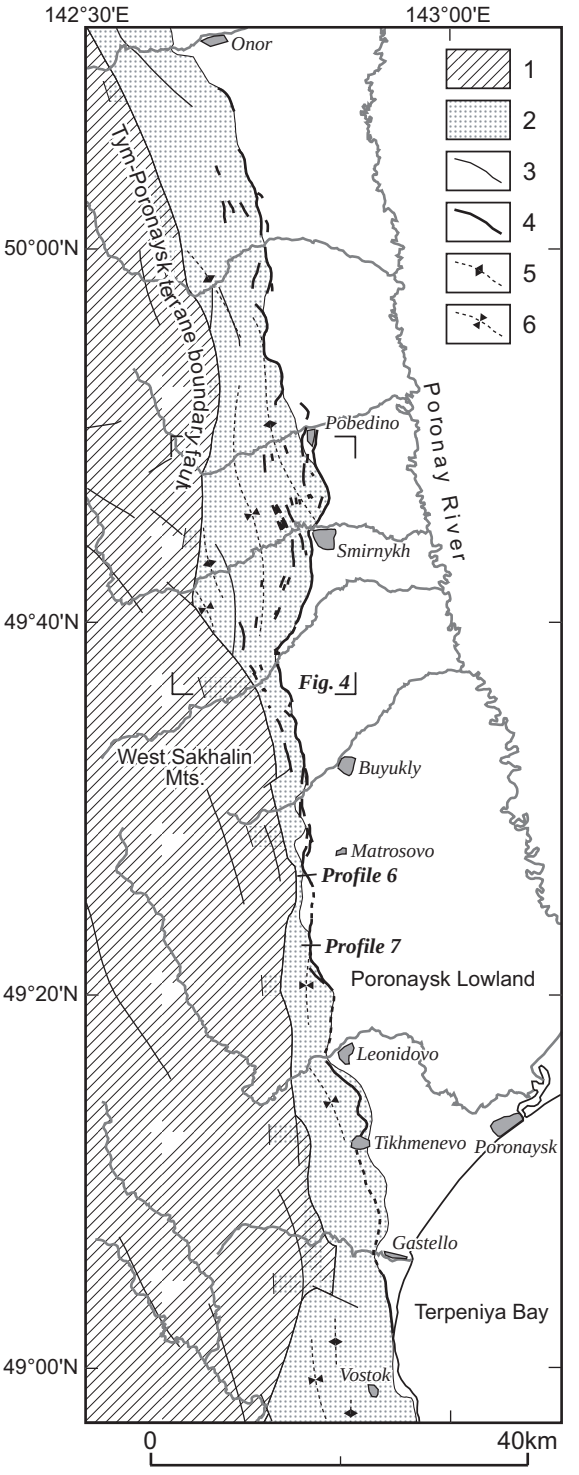

Fig. 3. Distribution of active faults along the western margin of the Poronaysk Lowland. See Fig. 2 for location of the figure. Geology is based on Bulgakov et al. (2002). 1: Upper Cretaceous strata, 2: Neogene strata, 3: inactive faults, 4: active faults, 5: anticlinal axis, 6: synclinal axis. Locations of topographic profiles 6 and 7 in Fig. 5 are also shown.

3. Active faulting along the western margin of the Poronaysk Lowland

3.1. Distribution and age of geomorphic surfaces

Fluvial terraces are well developed along the western margin of the Poronaysk Lowland and are displaced by the active strands of the Tym–Poronaysk fault (Figs. 3, 4). The terrace deposits were formed by east-flowing rivers from the West Sakhalin Mountains, which are tributaries of the Poronay River flowing into Terpeniya Bay. Using aerial photographs, we classified these terraces into H, M1, M2, L1, and L2 terraces in descending order, based on relative height from the present river channels and degree of dissection. Fig. 4 shows the distribution of terraces and active faults near the City of Smirnykh, where we have conducted extensive geomorphic and paleoseismic studies. Most terraces develop west of the active strands of the Tym–Poronaysk fault, suggesting that the uplift of the western block of the active faults plays an important role in development of the terraces. Among the five terraces, L1 terrace is most widely distributed in the study area. L2 terrace is a strath terrace cutting into L1 terrace along the present river channels such as the Orlovka and Yel'naya Rivers in the Smirnykh area (Fig. 4). As described below, radiocarbon ages for gravels and overbank deposits of L2 terrace exposed during trench excavations north of Smirnykh indicate that L2 terrace is of middle Holocene age. Although we could not obtain a radiometric age for L1 terrace, we tentatively estimate the age of L1 terrace to be the last glacial maximum at about 20 ka, based on similarity in geomorphic features to well-dated terraces in Hokkaido Island. During the last glacial period, periglacial processes were much more active than today, and thus debris supply from mountainous areas was much greater. This led to formation of widely developed fill terraces at ~20 ka in northern Japan (Koaze et al., 2003). In addition, L2 terrace of middle Holocene age is about 5 m above the flood plain of the Orlovka River, whereas L1 terrace is about 20 m higher than the flood plain. We have no data on the age of the higher terraces.

3.2. Distribution of active faults and their tectonic geomorphic features

Along the western margin of the Poronaysk Lowland, active faults are distributed from near Vostok at latitude 49°N northward to near Onor at latitude 50°10′N (Fig. 3). These active faults are classified into two categories. The easternmost faults are continuous and mark a boundary between Neogene strata and the alluvial plain, and the faults to the west are short and parallel to bedding planes. We interpret the former as the main trace of the active strand of the Tym–Poronaysk fault and the latter as flexural-slip faults on the hanging wall of the main fault. The surface trace of the active strand of the Tym–Poronaysk fault lies east of the terrane boundary fault; they are only 1 km apart near Matrosovo, whereas they are 13 km apart near Smirnykh (Fig. 3). The Tym–Poronaysk terrane boundary fault is a moderately west-dipping fault (Rozhdestvenskiy, 1982; Fournier et al., 1994). We found an exposure of the active strand of the Tym–Poronaysk fault along the Yel'naya River, where the fault dips 30°W and offset the base of L1 terrace gravel about 15 m (Fig. 4). Tectonic geomorphic features along the active strand include down-to-the-east fault scarps, eastward monoclinal warping, and westward tilting of fluvial terraces, which are typical geomorphic features along west-dipping reverse faults. We could not identify geomorphic evidence for strike-slip movement on the active strand. In contrast, the Tym–Poronaysk terrane boundary fault is interpreted to be inactive because the fault does not offset L1 terrace on the Orlovka River (Fig. 4). These data suggest that Quaternary movement of the Tym–Poronaysk fault is taken up by the active strand that has migrated basinward for 1–13 km from the terrane boundary fault.

We have taken topographic profiles across the fault scarps along the active stand of the Tym–Poronaysk fault (Fig. 5). Fault scarps on L2 terrace are 4–7 m high, those on L1 terrace are 18–27 m high, and the total elevation difference on M2 terrace is up to 70 m. Larger displacements on progressively older terraces indicate that the fault has ruptured repeatedly in the late Quaternary. Assuming the age of L1 terrace to be 20 ka, the vertical component of slip rate of the active strand of the Tym–Poronaysk fault is calculated as 0.9–1.4 mm/year. The dip of the fault on an outcrop and trench walls described below is 30–60°W. These values give a net slip rate of 1.0–2.8 mm/year for the active strand of the Tym–Poronaysk fault.

Northward from Pobedino, faulted geomorphic features gradually become obscured and the fault terminates near Onor (Fig. 3). To the south, we can trace the fault south to near Vostok, where the fault trace extends offshore. The length of the active strand of the Tym–Poronaysk fault on land is about 140 km. Southward from Vostok, we cannot directly trace the main fault, but we can trace secondary flexural-slip faults at least to

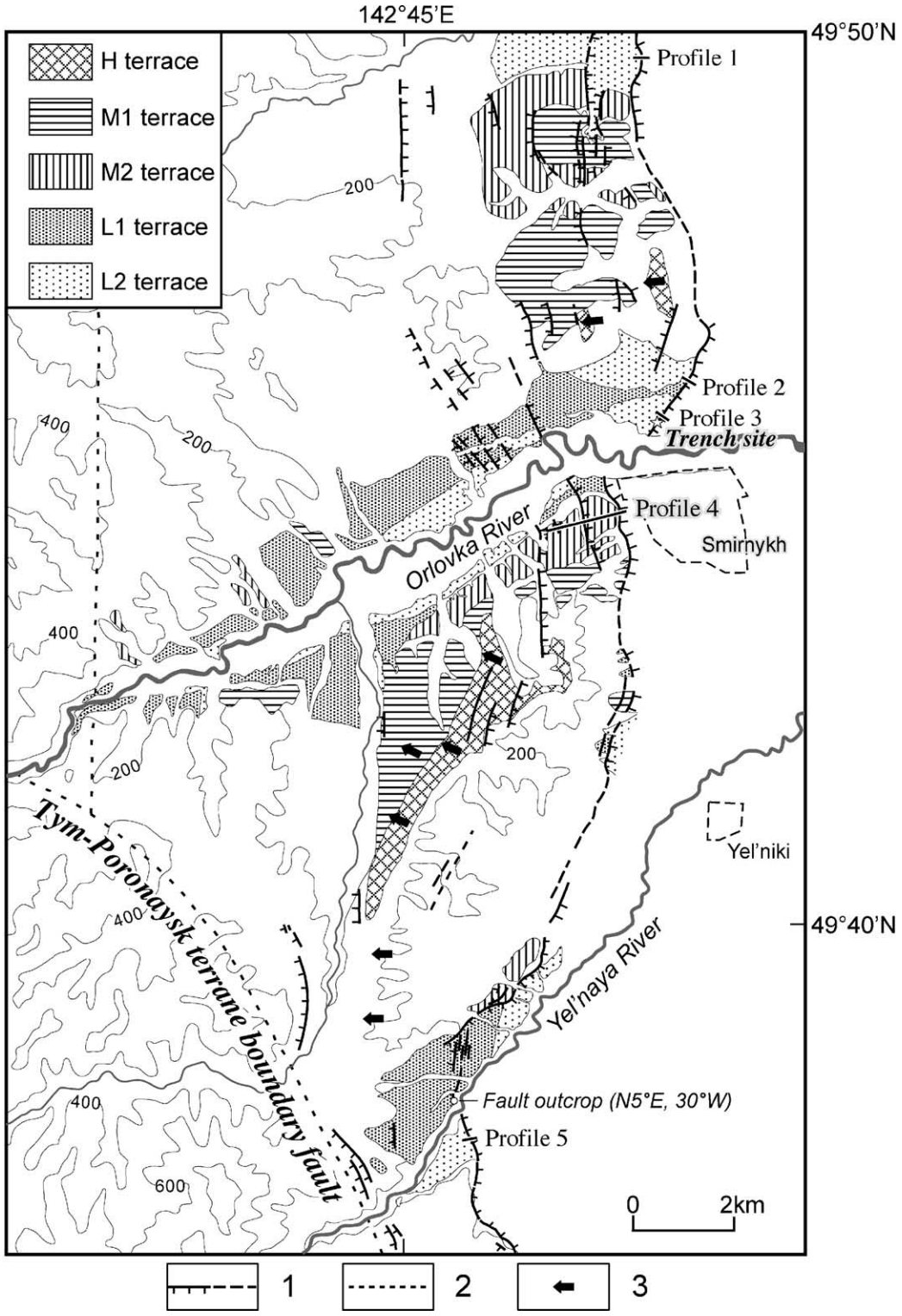

Fig. 4. Map showing classification of fluvial terraces and traces of active faults near Smirnykh based on aerial photograph interpretation and field observations. Contour interval is 200 m. Locations of topographic profiles 1 through 5 in Fig. 5 are also shown. Explanations for tectonic features are 1, active fault traces (dashed where location is uncertain; bars on downthrown side); 2, inactive Tym–Poronaysk terrane boundary fault; 3, back tilting of fluvial terraces.

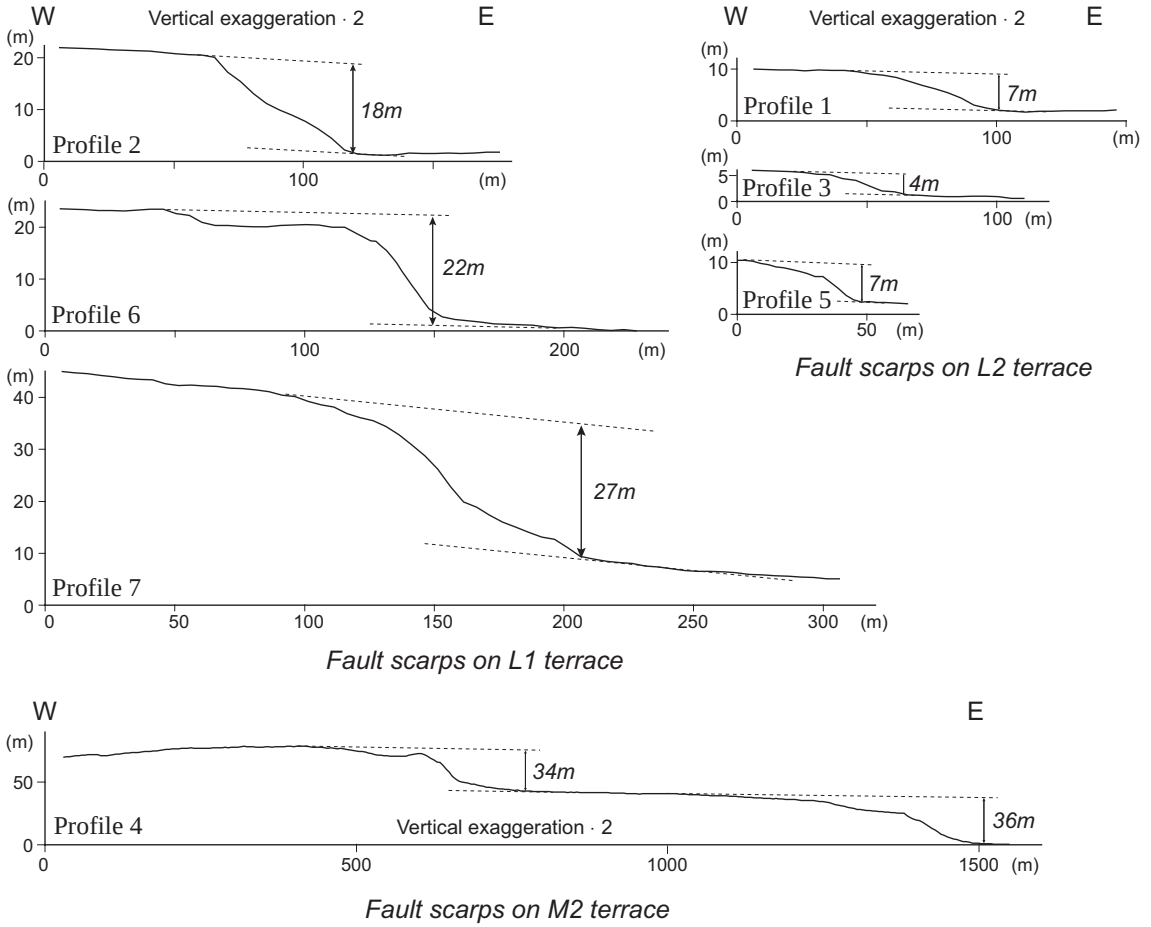

Fig. 5. Topographic profiles across the tectonic scarps along the active strand of the Tym–Poronaysk fault. Locations of the profiles are shown in Figs. 3 and 4.

Makarov (Fig. 2). Most of the secondary faults are identified as down-to-the-west scarps and some of them offset marine terraces. In addition, the western shore of Terpeniya Bay is characterized by uplifted marine terraces, which might be evidence for late Quaternary movement of the offshore Tym–Poronaysk fault. Along the western margin of the Yuzhno–Sakhalinsk Lowland, the Tym–Poronaysk fault also shows geomorphic evidence for late Quaternary activity (Suzuki et al., 2000; Bulgakov et al., 2002). Kariya et al. (2000) excavated a trench across the Tym–Poronaysk fault about 40 km southwest of Yuzhno–Sakhalinsk and identified west-dipping reverse faults that cut fluvial deposits dated at 32–42 ka. The vertical component of slip rate was estimated at 0.05–0.08 mm/year or greater. Farther to the south across the Soya Strait, there is no major west-dipping faults that could be an extension of the Tym–Poronaysk fault. Instead, the Teshio fault zone forms a west-verging fold-and-thrust belt (Fig. 2) and most of east-west convergence in northern Hokkaido appears to be taken up by this structure (Ikeda et al., 2002).

4. Paleoseismic trenching north of Smirnykh

In order to obtain data on paleoseismic activity of the active strand of the Tym–Poronaysk fault, we excavated two trenches 100 m apart about 1 km north of downtown Smirnykh (Fig. 4). The 20-m-long and 4.5-m-deep southern trench was excavated across a 4-m-high fault scarp on L2 terrace, but the fault was not exposed on the trench walls. This was because the original fault scarp was eroded westward more than 5 m by the Orlovka River. We then excavated another trench about 100 m to the north, away from the river channel, and clear fault zones were exposed on the trench walls. This northern trench was 16 m long and 3.5 m deep across a fault scarp about 4 m high on L2 terrace (Fig. 6). The trench was oriented N25°W, almost perpendicular to the fault trace. The lower half of the

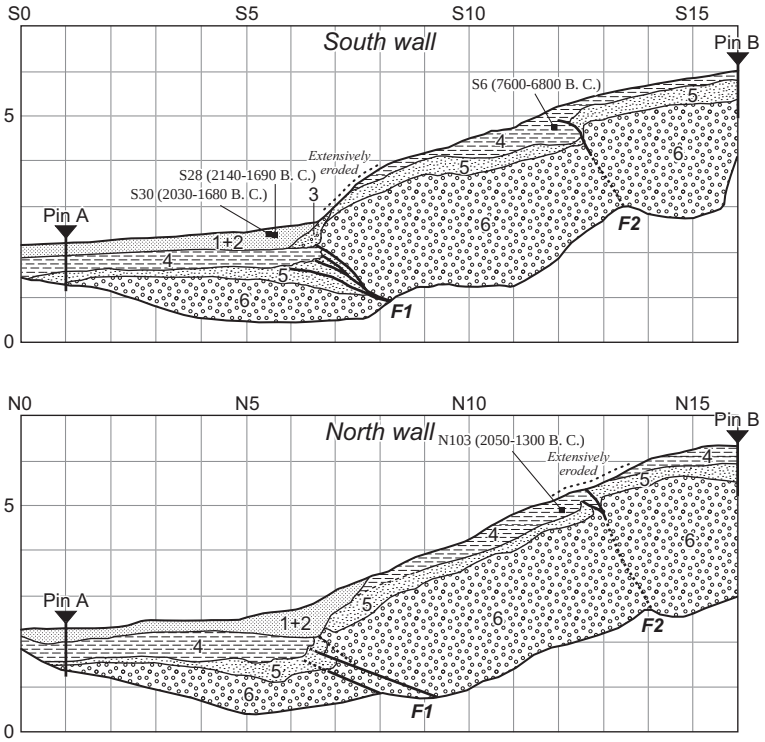

Fig. 6. Simplified logs of the south and north walls of the trench north of Smirnykh. Grid interval is 1 m. Numerals denote stratigraphic units. Calibrated ages for charcoal samples are also shown. Location of the trench site is shown in Fig. 4.

trench wall is almost vertical but the upper half slopes as low as 60°; we projected stratigraphic features onto a vertical plane during logging. Prior to the excavation, the trench site was densely forested. We first removed trees using a bulldozer and then excavated the trench by a backhoe. During the removal of vegetation, surface soils as much as 20–30 cm thick were removed but it does not affect our interpretation on the timing and displacement of paleoseismic events.

We have logged the north and south walls at a scale of 1:40 (Fig. 6). Near the main fault zone (F1), we logged both walls at a scale of 1:10 (Fig. 7). We then collected charcoal and wood fragments for radiocarbon dating. The samples were dated at National Institute of Environmental Studies, Japan (laboratory code: NIES) and Tono Geoscience Center, Japan Nuclear Cycle Development Institute (laboratory code: GX).

4.1. Stratigraphy

The strata exposed on the trench walls are fluvial deposits of the Orlovka River (Fig. 6). We divided the strata into 6 units based on lithology and relationship with faulting events. We describe these strata from the lower stratigraphic horizon.

Unit 6 consists of clast-supported gravel layers of L2 terrace. The gravel layers are composed of well-rounded Cretaceous sandstone and siltstone clasts with a maximum diameter of 20 cm. Lenses of coarse sand are contained within the gravel layers (Fig. 7). This unit is at least 2.5 m thick because the base of the gravels was not exposed on the trench walls. We could not find a datable material from unit 6 in this trench. However, a wood fragment obtained 2 m below the top of gravel layers of L2 terrace in the southern trench was dated at 6540 ± 90 years BP (GX-2052) that is calibrated to a 2σ calendar age of 5630–5320 B. C.

Units 4 and 5 are overbank sand deposits overlying the terrace gravels. We divided the overbank deposit into two units based on degree of soil development. Unit 5 is composed of grayish-yellow medium to coarse sands with lenses of granules. This unit maintains a constant thickness of 20–30 cm, except for between S6 and S7 where the unit is as much as 80 cm thick because of stacking of the strata by reverse faulting along F1 (Fig. 7).

Unit 4 is dark brown, 40–60-cm-thick, clay rich B horizon of Podzol, typical soil sequence in central and northern Sakhalin. On the hanging wall side of F1, top of this unit was eroded during removal of trees prior to

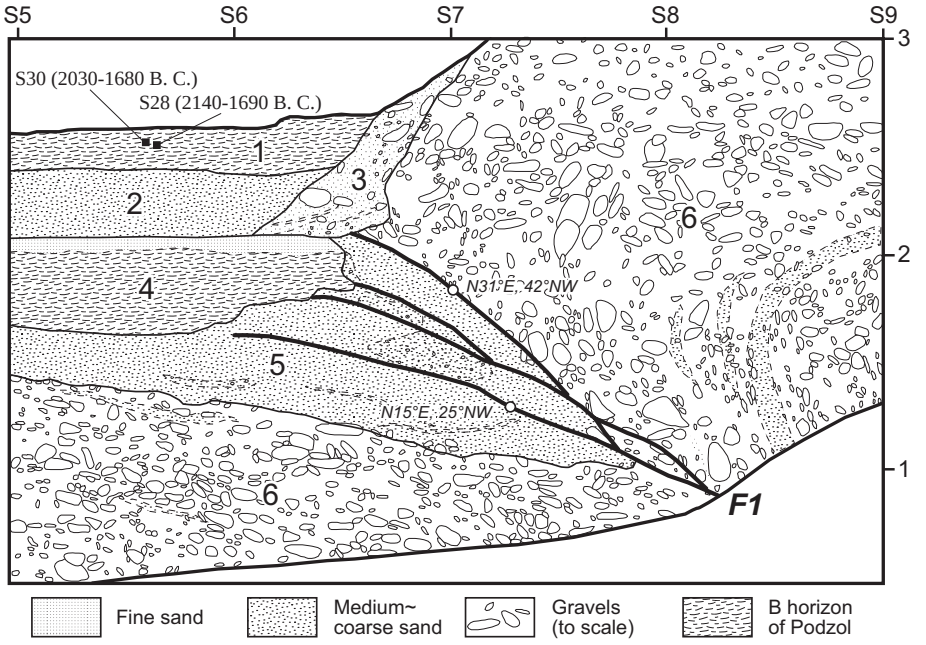

Fig. 7. Detailed log around F1 on the south wall. Numerals denote stratigraphic units. Calibrated ages for charcoal samples are also shown.

the excavation (Fig. 6). On the downthrown side, the topmost 5–10 cm of unit 4 is pale yellow, hard, fine sand that may be correlated to the A horizon of Podzol. Thus, the top of unit 4 seems to have been at the ground surface for an extended amount of time. We have obtained two ^{14}C ages from unit 4 (Fig. 6, Table 1). The age from the south wall is 7600–6800 B. C., whereas the age from the north wall is 2050–1300 B. C. Considering the age from unit 6 is about 5500 B. C., the age obtained from the south wall appears to be too old for unit 4 and we interpreted that the charcoal was reworked from its original depositional position.

Unit 3 is a colluvial wedge deposit at the base of the monoclinal scarp (Figs. 6, 7). This deposit is composed of a mixture of gravels from unit 6 and medium to coarse sands from units 4 and 5. The wedge shape and its location at the base of the monoclinal scarp indicate that this is a post-faulting colluvial deposit. This colluvial wedge is clearly recognized on the south wall, while it is not clearly defined on the north wall.

Units 1 and 2 are present only on the downthrown side of F1. Unit 2 is medium to coarse sand with lenses of granules. This deposit onlaps the colluvial wedge deposit of unit 3 (Fig. 7). The topmost part of this unit is brownish, humic soil, correlated to the O horizon of Podzol. However, A and B horizons have not developed in this unit.

Unit 1 is dark yellow fine sand to silt, correlated to the B horizon of the modern soil profile. From the upper part of this unit on the south wall, we obtained two ^{14}C ages around 2000–1700 B. C. (Figs. 6 and 7).

Table 1
AMS ^{14}C dates for samples from the Smirnykh trench

Sample number[a]	Laboratory number[b]	Sampled unit	Trench grid location (horizontal/vertical)	^{14}C Age (years BP)[c]	Calibrated age B. C. (2σ)[d]
S6	NIES2012	4	S11.94/4.88	8260 ± 130	7600–6800
S28	NIES2019	1	S5.65/2.52	3560 ± 70	2140–1690
S30	NIES2020	1	S5.60/2.53	3510 ± 70	2030–1680
N103	NIES2021	4	N12.18/4.88	3360 ± 130	2050–1300

[a] All samples are detritus charcoal.
[b] Samples were processed at AMS facility at National Institute of Environmental Studies, Japan (NIES). Samples were pretreated with standard acid and base wash.
[c] Ages were not $\delta^{13}C$ corrected.
[d] OxCal version 3.9 software was used for calibration.

4.2. Fault structures

Two fault zones, F1 and F2, were exposed on the trench walls (Fig. 6). F1 is interpreted as the primary fault zone based on its location at the base of the tectonic scarp and a large amount of stratigraphic offset. F1 consists of several fault strands, which dip 25–45°NW. F1 thrusts gravels of unit 6 over sands of unit 5 (Fig. 7). While the westernmost strand of F1 on the south wall extends upward to a paleo-surface marked by the top of unit 4, the other strands do not propagate through unit 4. This is probably because unit 4 was too cohesive to be cut by the faults and/or the slip on each fault is smaller than the westernmost fault. F1 is overlain by undeformed colluvial wedge deposit of unit 3, suggesting that the most recent surface-rupturing event occurred after the deposition of unit 4 and before the deposition of unit 3. F1 not only cuts units 4, 5, and 6 but also folds the strata on the hanging wall of the fault. Clasts and sand lenses in unit 6 were folded into a monocline; they are deformed almost vertical or overturned within a few meters of the fault zone (Fig. 7). This demonstrates that the scarp we excavated is a monoclinal or fold scarp rather than a fault scarp.

F2 is a reverse fault on the hanging wall side of F1. This fault dips to the west at 60–70°. It offsets the tops of units 5 and 6 about 20–30 cm but terminates within unit 4 on the south wall. This abrupt termination of F2 seems to be also related to cohesiveness of unit 4. F2 is recognized as a zone of reorientation of clasts within the gravels of unit 6. Based on fault geometry, we speculate that oblique-slip may be partitioned into dip-slip on F1 and strike-slip on F2. We, however, do not have geomorphic evidence for strike-slip faulting along the active strand of the Tym–Poronaysk fault, although GPS data detect dextral oblique-convergence across the fault zone (Kogan et al., 2003).

4.3. Age and displacement of the most recent faulting event

On the trench walls, we are able to identify stratigraphic evidence for only the most recent faulting event. Thus the 4-m-high tectonic scarp on L2 terrace at the trench site resulted from one faulting event. As described above, the event occurred after the deposition of unit 4 and before the deposition of unit 3. We obtained a calibrated age of 2050–1300 B. C. from unit 4. We could not date unit 3 but obtained two ages of 2140–1690 B. C. and 2030–1680 B. C. from unit 1 (Fig. 6, Table 1). These ages constrain the timing of the most recent faulting event between 2050 B. C. and 1690 B. C.

Stratigraphic separation of the top of unit 6 by F1 on the south wall is about 1.5 m and that by F2 is about 20 cm. These values are too small to explain the height of the tectonic scarp. However, as we previously noted, the strata were folded to a monocline and a large portion of fault displacement is consumed by folding of the hanging wall strata. We calculated the net slip during the most recent faulting event using a retro-deformation technique used by Schneider et al. (1996) (Fig. 6, Table 2). We put pin A at S1 and N1 and pin B at S16 and N16, both well outside the deformation zone. The distance between the pins is 15.0 m on the both walls. We then measured the length along the top of unit 6 between pins A and B using a curvimeter: 17.6 m on the south wall and 17.0 m on the north wall. Since the top of unit 6 was supposed to have been almost flat, the differences between the values above represent horizontal shortening associated with reverse faulting during the most recent event: 2.6 m on the south wall and 2.0 m on the north wall. The vertical displacements on the top of unit 6 are 3.6 m on the south wall and 4.0 m on the north wall. Using trigonometry, net slips are calculated as 4.4 m on the south wall and 4.5 m on the north wall. The dips of the fault are calculated as 54° and 63°, slightly steeper than the dips of F1 on the trench walls.

5. Discussion

The active strand of the Tym–Poronaysk fault along the western margin of the Poronaysk Lowland has moved repeatedly in late Quaternary time and poses serious seismic hazards to central Sakhalin. The length of the fault zone onshore is about 140 km. If the fault moves along its entire length in a single earthquake, it would produce a M_w 7.6 earthquake based on empirical relations by Wells and Coppersmith (1994). This mag-

Table 2
Calculation of net slip associated with the most recent faulting event at the Smirnykh trench site

Trench wall	Distance between pins A and B	Length along top of unit 6	Horizontal shortening during MRE	Vertical displacement on top of unit 6	Net slip during MRE	Dip of fault
South	15.0 m	17.6 m	2.6 m	3.6 m	4.4 m	54°
North	15.0 m	17.0 m	2.0 m	4.0 m	4.5 m	63°

nitude is almost comparable to the magnitudes of historical earthquakes along the Eurasian/Okhotsk plate boundary to the south (Fig. 1). We, however, need additional geologic and paleoseismic data to identify portions of the fault zone that rupture simultaneously in a single earthquake.

We have tentatively estimated a net-slip rate of 1.0–2.8 mm/year for the fault. This slip rate is comparable to those of major reverse faults in northern Japan (Research Group for Active Faults of Japan, 1991). The last surface-rupturing earthquake at the Smirnykh trench site occurred about 3500–4000 years ago. These data suggest that strain in a range of 3.5–11 m has accumulated across the fault zone. Because the slip during the most recent event was estimated to be about 4.5 m, the potential for a large earthquake along the active strand of the Tym–Poronaysk fault in central Sakhalin is high.

A net slip rate of 1.0–2.8 mm/year translates into a 0.5–2.4 mm/year convergence rate as the fault dips 30–60°W. The upper bound of our estimate is close to ~3 mm/year of convergence rate determined by GPS measurements (Kogan et al., 2003) and ~2 mm/year of convergence rate between the Eurasian and Okhotsk plates predicted by the plate model of Seno et al. (1996). According to Seno et al. (1996), the Eurasian/Okhotsk Euler pole is located west of Okha in northern Sakhalin (Fig. 1) and the Okhotsk plate rotates clockwise relative to the Eurasian plate. This model well explains the right-lateral shear zone in northern Sakhalin and east-west convergence in central and southern Sakhalin (Fig. 2). This model also predicts a larger convergence rate to the south, away from the pole of rotation. However, slip rate data along the plate boundary offshore are sparse. Instead, we can compare recurrence intervals of large earthquakes estimated by trenching on land and earthquake-triggered turbidite studies offshore. The last surface-rupturing earthquake at the Smirnykh trench site was 3500–4000 years ago. The Ekhabi–Pil'tun fault in northern Sakhalin ruptured only twice in the past 7500 years (Tsutsumi et al., 2000). At the Rishiri Trough west of the Soya Strait, Ikehara (2000) dated the last and penultimate seismic events at 2300 and 5500 years ago based on analysis of turbidite deposits. Thus in and around Sakhalin, the recurrence intervals of major active faults are ~3000 years or longer. Farther to the south, the faults at the plate boundary have shorter recurrence intervals. Near the epicentral area of the 1993 Hokkaido–Nansei-oki earthquake, the recurrence interval of a similar earthquake is 1000–1500 years (Shimokawa and Ikehara, 2002). South of the 1964 Niigata earthquake area, the plate boundary extends onshore as the Shinano River fold-and-thrust belt. The recurrence intervals of the faults there are estimated at 1000–2000 years (e.g. Watanabe et al., 2000). This southward increase of fault activity along the plate boundary supports the plate model of Seno et al. (1996). In conclusion, active fault and paleoseismic data support the plate model by Seno et al. (1996) that was originally proposed based on seismicity and earthquake slip vectors.

6. Conclusion

We have studied active faulting along the western margin of the Poronaysk Lowland in central Sakhalin, which lies on an active plate boundary between the Okhotsk and Eurasian plates. Based on aerial photograph interpretation and field observations, we have mapped a 140-km-long active fault zone. These active faults are located east of and parallel to the Tym–Poronaysk fault, a terrane boundary between Upper Cretaceous and Neogene strata, and appear to have reactivated the terrane boundary at depth in Quaternary time. Tectonic geomorphic features such as east-facing monoclinal and fault scarps, back-tilting of fluvial terraces, and numerous secondary faults suggest that the faults are west-dipping reverse faults. Assuming the most widely developed geomorphic surface (L1) in the study area formed during the last glacial maximum at about 20 ka, we obtain a vertical component of slip rate of 0.9–1.4 mm/year. Using the fault dip of 30–60°W observed at an outcrop and trench walls, a net slip rate of 1.0–2.8 mm/year is obtained. The upper bound of the estimate is close to a convergence rate across the Tym–Poronaysk fault based on GPS measurements. A trenching study across the fault zone revealed the timing of the most recent faulting event at 3500–4000 years ago. The net slip associated with the event is estimated at about 4.5 m. Since the last faulting event, a minimum of 3.5 m of strain, close to the strain released during the last event, has accumulated along the central portion of the active strand of the Tym–Poronaysk fault. The sense of slip and convergence rate of the active strand of the Tym–Poronaysk fault is consistent with a plate model proposed by Seno et al. (1996).

Acknowledgements

This research was supported by grants from the Ministry of Education, Culture, Sports, Science, and Technology of Japan and Fukutake Science and Culture Foundation. Gaku Kimura, Toshihiko Shimamoto, and

Alexei I. Ivashchenko initiated a joint research project on active tectonics in Sakhalin between Russian and Japanese scientists. We thank Mitsuhisa Watanabe, Daisuke Hirouchi and Tatsuya Ishiyama for helpful discussion during aerial photograph interpretation. We also thank the staff at Institute of Marine Geology and Geophysics, Russian Academy of Sciences for logistic support. Thanks are also due to Nikolai Terentief, the director of the Far-East Geological Information Center in Yuzhno–Sakhalinsk, for his cooperation during aerial photograph interpretation at the center. Comments from Mike Sandiford and two anonymous reviewers are greatly appreciated. Constructive review by Robert S. Yeats on an early version of the manuscript has greatly improved the paper. Shaded relief map in Fig. 2 was drawn with the GMT software (Wessel and Smith, 1998). OxCal software was used for calibration of radiocarbon ages.

References

Arefiev, S., Rogozhin, E., Tatevossian, R., Rivera, L., Cisternas, A., 2000. The Neftegorsk (Sakhalin Island) 1995 earthquake: a rare interplate event. Geophys. J. Int. 143, 595–607.

Bulgakov, R.F., Ivashchenko, A.I., Kim, C.U., Sergeev, K.F., Strel'tsov, M.I., Kozhurin, A.I., Besstrashnov, V.M., Strom, A.L., Suzuki, Y., Tsutsumi, H., Watanabe, M., Ueki, T., Shimamoto, T., Okumura, K., Goto, H., Kariya, Y., 2002. Active faults in northeastern Sakhalin. Geotectonics 36, 227–246.

Fournier, M., Jolivet, L., Huchon, P., Sergeyev, K.F., Oscorbin, L.S., 1994. Neogene strike-slip faulting in Sakhalin and the Japan Sea opening. J. Geophys. Res. 99, 2701–2725.

Ikeda, Y., Imaizumi, T., Togo, M., Hirakawa, K., Miyauchi, T., Sato, H. (Eds.), Atlas of Quaternary Thrust Faults in Japan. Univ. Tokyo Press, Tokyo. 254 pp. (in Japanese).

Ikehara, K., 2000. Large earthquakes recorded as deep-sea turbidites in the Rishiri Trough, northernmost Hokkaido. Quat. Res. 39, 569–574 (in Japanese with English abstract).

Ivashchenko, A.I., Kim, C.U., Oscorbin, L.S., Poplavskaya, L.N., Poplavsky, A.A., Burymskaya, R.N., Mikhailova, T.G., Vasilenko, N.F., Streltsov, M.I., 1997. The Neftegorsk, Sakhalin Island, earthquake of 27 May 1995. Isl. Arc 6, 288–302.

Jolivet, L., Miyashita, S., 1985. The Hidaka shear zone (Hokkaido, Japan): genesis during a right-lateral strike-slip movement. Tectonics 4, 289–302.

Kariya, Y., Bulgakov, R.F., Shimokawa, K., 2000. Trenching study on the Taranay fault in south Sakhalin, far eastern Russia. J. Geogr. 109, 302–310 (in Japanese with English abstract).

Katsumata, K., Kasahara, M., Ichiyanagi, M., Kikuchi, M., Sen, R.S., Kim, C.U., Ivaschenko, A., Tatevossian, R., 2004. The 27 May 1995 Ms 7.6 northern Sakhalin earthquake: an earthquake on an uncertain plate boundary. Bull. Seismol. Soc. Am. 94, 117–130.

Kimura, G., Miyashita, S., Miyasaka, S., 1983. Collision tectonics in Hokkaido and Sakhalin. In: Hashimoto, M., Uyeda, S. (Eds.), Accretion Tectonics in the Circum-Pacific Regions. Terrapub, Tokyo, pp. 123–134.

Koaze, T., Nogami, M., Ono, Y., Hirakawa, K. (Eds.), Geomorphology of Hokkaido, Regional Geomorphology of the Japanese Islands, vol. 2. Univ. Tokyo Press, Tokyo. 359 pp. (in Japanese).

Kogan, M.G., Bürgmann, R., Vasilenko, N.F., Scholz, C.H., King, R.W., Ivashchenko, A.I., Frolov, D.I., Steblov, G.M., Kim, C.U., Egorov, S.G., 2003. The 2000 Mw 6.8 Uglegorsk earthquake and regional plate boundary deformation of Sakhalin from geodetic data. Geophys. Res. Lett. 30, 1102, doi:10.1029/2002GL016399.

Research Group for Active Faults of Japan, 1991. Active Faults in Japan- Sheet Maps and Inventories (revised edition). Univ. Tokyo Press, Tokyo, 437 pp. (in Japanese with English abstract).

Rogozhin, E.A., 1996. Focal mechanism of the Neftegorsk, Sakhalin earthquake of May 27 (28), 1995. Geotectonics 30, 124–131.

Rozhdestvenskiy, V.S., 1982. The role of wrench-faults in the structure of Sakhalin. Geotectonics 16, 323–332.

Schneider, C.L., Hummon, C., Yeats, R.S., Huftile, G.L., 1996. Structural evolution of the northern Los Angeles basin, California, based on growth strata. Tectonics 15, 341–355.

Seno, T., Sakurai, T., Stein, S., 1996. Can the Okhotsk plate be discriminated from the North American plate? J. Geophys. Res. 101, 11305–11315.

Shimamoto, T., Watanabe, M., Suzuki, Y., Kozhurin, A.I., Strel'tsov, M.I., Rogozhin, E., 1996. Surface faults and damage associated with the 1995 Neftegorsk earthquake. J. Geol. Soc. Jpn. 102, 894–907 (in Japanese with English abstract).

Shimokawa, K., Ikehara, K., 2002. Paleoearthquakes recorded in sediments. In: Ohtake, M., Taira, A., Ota, Y. (Eds.), Active Faults and Seismo-Tectonics of the Eastern Margin of the Japan Sea. Univ. Tokyo Press, Tokyo, pp. 95–108 (in Japanese).

Suzuki, Y., Tsutsumi, H., Watanabe, M., Ueki, T., Okumura, K., Goto, H., Strel'tsov, M.I., Kozhurin, A.I., Bulgakov, R., Terentief, N., Ivashchenko, A.I., 2000. Preliminary report on active faults in Sakhalin, Russia. J. Geogr. 109, 311–317 (in Japanese with English abstract).

Tsutsumi, H., Kozhurin, A.I., Strel'tsov, M.I., Ueki, T., Suzuki, Y., Watanabe, M., 2000. Active faults and paleoseismology in northeastern Sakhalin, Russia. J. Geogr. 109, 294–301 (in Japanese with English abstract).

Watanabe, M., Ota, Y., Suzuki, I., Sawa, H., Suzuki, Y., 2000. Holocene activity and timing of the latest faulting event of the Torigoe fault, west of Nagaoka City, central Japan. J. Seismol. Soc. Jpn. 53, 153–164 (in Japanese with English abstract).

Wells, D.L., Coppersmith, K.J., 1994. New empirical relationships among magnitude, rupture length, rupture width, rupture area, and surface displacement. Bull. Seismol. Soc. Am. 84, 974–1002.

Wessel, P., Smith, W.H.F., 1998. New, improved version of Generic Mapping Tools released. EOS Trans. AGU 79, 579.

Yeats, R.S., 1986. Active faults related to folding. Active Tectonics. Nat. Acad. Press, Washington, DC, pp. 63–79.